

# Broad primordial power spectrum and $\mu$ -distortion constraints on primordial black holes

Zhan-He Wang<sup>1,2\*</sup>, Hai-Long Huang<sup>1,2†</sup>, and Yun-Song Piao<sup>1,2,3,4‡</sup>

<sup>1</sup> *School of Fundamental Physics and Mathematical Sciences,  
Hangzhou Institute for Advanced Study, UCAS, Hangzhou 310024, China*

<sup>2</sup> *School of Physical Sciences, University of Chinese  
Academy of Sciences, Beijing 100049, China*

<sup>3</sup> *International Center for Theoretical Physics Asia-Pacific, Beijing/Hangzhou, China and*

<sup>4</sup> *Institute of Theoretical Physics, Chinese Academy of Sciences,  
P.O. Box 2735, Beijing 100190, China*

## Abstract

Supermassive black holes (SMBHs) might originate from supermassive primordial black holes (PBHs). However, the hypothesis that these PBHs formed through the enhancement of the primordial curvature perturbations has consistently faced significant challenges due to the stringent constraints imposed by  $\mu$ -distortion in the cosmic microwave background (CMB). In this work, we investigate the impact of non-Gaussianity on  $\mu$ -distortion constraint in the context of broad power spectra. Our results show that, under the assumption of non-Gaussian curvature perturbations, a broad power spectrum may lead to weaker  $\mu$ -distortion constraints compared to the Gaussian cases. Our findings highlight the potential of the broad power spectrum to alleviate the  $\mu$ -distortion constraints on supermassive PBHs under large non-Gaussianity.

---

\* [wangzhanhe19@mailsucas.ac.cn](mailto:wangzhanhe19@mailsucas.ac.cn)

† [huanghailong18@mailsucas.ac.cn](mailto:huanghailong18@mailsucas.ac.cn)

‡ [yspiao@ucas.ac.cn](mailto:yspiao@ucas.ac.cn)

## I. INTRODUCTION

Primordial black holes (PBHs), first proposed by Refs. [1–3], could have formed in the early Universe from the collapse of high-density regions due to primordial fluctuations. Then the PBHs has been a subject of extensive research in cosmology, with implications for dark matter (DM) [4–9], and supermassive black holes (SMBH) residing in galactic nuclei [10, 11], see also recent reviews [12–21]. More recently, it has been showed that the merger of supermassive PBHs (SMPBHs) ( $10^{6-10} M_{\odot}$ )<sup>1</sup> might be also the source of nano-Hertz gravitational wave background, e.g.[22–27]. The supermassive black holes (SMBHs) observed at high redshifts by the James Webb Space Telescope (JWST) are posing a challenge to the  $\Lambda$ CDM model [27–32].

However, the scenario of SMPBHs is strongly constrained by spectral distortions in the CMB due to an enhanced dissipation of acoustic waves. Specifically, although the CMB photon spectrum is expected to follow a perfect blackbody radiation spectrum [33–35], small deviations can be caused by injecting extra energy into the photon bath or altering the photon number density [36–39]. The corresponding mechanisms include the dissipation of acoustic waves, the adiabatic cooling of electrons, the injection of energy through Hawking evaporation and accretion of PBHs in the early universe, and the Sunyaev-Zeldovich effect of galaxy clusters in the late universe [40–43]. According to different redshift intervals, the deviations can be classified into  $y$  ( $z \lesssim 5 \times 10^4$ ) and  $\mu$  ( $5 \times 10^4 \lesssim z \lesssim 2 \times 10^6$ ) - distortions. The redshift corresponding to the PBHs within the SMPBH mass range falls within the redshift range of  $\mu$ -distortion. Thus,  $\mu$ -distortion sets stringent constraints on the amplitude of the primordial power spectrum at the corresponding scales. It has been found that for the monochromatic primordial power spectrum, the maximal PBH mass permitted by the constraints of  $\mu$ -distortion is approximately  $10^4 M_{\odot}$  [44], while for the broad power spectrum the constraints will be strengthened [45, 46].

Currently, there are two main roads to avoid the  $\mu$ -distortion constraints: one is to consider a new PBH mechanism, different from large primordial perturbations that leads to collapse [22, 23, 47, 48]<sup>2</sup>, and the other is to consider large non-Gaussianity of primordial

---

<sup>1</sup> In principle, the mass range of a PBH can extend from  $10^{-18} M_{\odot}$  to  $10^{16} M_{\odot}$ . Those smaller than  $10^{-18} M_{\odot}$  would have evaporated by now due to Hawking radiation, or see recent [8, 9].

<sup>2</sup> In a landscape with multiple anti-de Sitter (AdS) vacua, AdS bubbles can collapse into PBHs [49, 50],

perturbations [24, 57–62]. In this paper, we still focus on the latter. Non-Gaussianity in the primordial power spectrum can significantly enhance the probability to form PBHs due to enhanced tail distributions [63]. Therefore, it plays a crucial role in setting the abundance of PBHs in various mass ranges, directly impacting their viability as DM candidates and as potential seeds for SMBHs [64, 65]<sup>3</sup>. The  $\mu$ -distortion constraints on monochromatic power spectrum with non-Gaussianities have been studied in [24, 57, 60].

However, the  $\mu$ -distortion constraint on broad power spectrum in the context of non-Gaussianity is still rare. In this paper, we investigate the  $\mu$ -distortion constraint on non-Gaussian broad log-normal (LN) and broken power law (BPL) power spectrum, which allow flexibility in modelling different inflationary scenarios [67], using the latest PBH abundance calculation method [59, 68, 69]. Unlike the monochromatic spectrum, where non-Gaussian effects amplify  $\mu$ -distortion constraints in large  $k$  space, we find that broad power spectrum can exhibit a weaker non-Gaussian  $\mu$ -distortion constraint (specifically the quadratic local non-Gaussianity) relative to Gaussian cases, especially as the spectrum is broader. This suggests that the interplay between spectral width and non-Gaussianity might have unexpected implications for the constraints of SMPBHs and requires further investigation.

This paper is outlined as follows. In [section II](#), we review the methods used to calculate PBH abundance and  $\mu$ -distortion constraints, by which we calculate and present  $\mu$ -distortion constraints for quadratic local non-Gaussianity using the log-normal power spectrum in [section III](#). In [section IV](#) we extend this calculation to the BPL power spectrum. We conclude in [section V](#) and our main results can be seen in [Table I](#).

## II. METHODS

### A. PBH abundance calculation

In this subsection, we present the calculation of PBH abundance for broad power spectrum in the non-Gaussian case, following [69]. A PBH forms when a sufficiently large primordial perturbation reenters the event horizon. The compaction function  $\mathcal{C}$  [70–72] is the most

---

which might be accompanied by a stochastic gravitational wave background, e.g. [51]. Thus it is also worth exploring whether AdS vacua in early universe, e.g. [52–56], can be relevant to the generation of SMPBHs.

<sup>3</sup> The non-Gaussianities have also a close relationship to PBH clustering leading to the potential to be tested by observation [66].

	$\delta$ -function	LN		BPL	
		$\Delta = 0.3$	$\Delta = 1$	(4, 10, 1)	(4, 3, 20)
Gaussian	4.25	3.83	2.55	3.67	2.63
NG ( $\kappa = 0.1$ )	4.28	3.98	2.63	3.83	2.77
NG ( $\kappa = 1$ )	4.31	4.22	3.54	4.07	3.42
NG ( $\chi^2$ )	4.47	4.25	4.00	4.01	3.67

TABLE I: The maximum PBH mass,  $\log \frac{M_{\text{PBH}}}{M_{\odot}}$ , allowed by  $\mu$ -distortion under the assumption  $f_{\text{PBH}} = 1$  for different types of primordial power spectrum:  $\delta$ -function (17), log-normal (16) and broken power law (28) form. We discuss the scenarios where primordial spectrum peaks obeying Gaussian and non-Gaussian statistics under the assumption of local (perturbative or not) non-Gaussianity. The parameter  $\kappa$  represents the strength of perturbative non-Gaussianity, defined as  $\tilde{f}_{\text{NL}}\sqrt{A_{\text{G}}}$ , and  $\chi^2$  represents non-perturbative non-Gaussianity. It can be seen from the table that the enhancement of non-Gaussianity relaxes the  $\mu$ -distortion constraints on the maximum PBH mass, and this trend becomes more pronounced as the power spectrum broadening increases. Thus, non-perturbative non-Gaussianity reduces the impact of power spectrum width on  $\mu$ -distortion constraints.

appropriate parameter for assessing whether the perturbation will collapse to form a PBH, and it is defined as

$$\mathcal{C}(r, t) \equiv 2 \frac{\delta M(r, t)}{R(r, t)}, \quad (1)$$

where  $\delta M(r, t)$  is the mass excess within a sphere areal radius  $R(r, t)$ ,  $r$  is the radius coordinate in the spherical coordinate. And the resulting PBH mass follows a critical scaling law [73, 74]

$$M_{\text{PBH}} = \mathcal{K} M_k (\mathcal{C} - \mathcal{C}_{\text{th}})^{\gamma}, \quad (2)$$

where

$$M_k \simeq 17 \left( \frac{g}{10.75} \right)^{-1/6} \left( \frac{k}{10^6 \text{ Mpc}^{-1}} \right)^{-2} M_{\odot} \quad (3)$$

is the Hubble horizon mass corresponding to a comoving scale  $k$ . Here,  $g$  is the number of relativistic degrees of freedom which equal to 10.75. The threshold  $\mathcal{C}_{\text{th}}$  can be estimated following [75] for different shapes of power spectrum. Furthermore, we fix  $\mathcal{K} = 4.4$  and  $\gamma = 0.38$  [76].

In the non-Gaussian case, in which the locally parameterization is  $\mathcal{R} = F(\mathcal{R}_G)$ , the compaction function can be characterized via its Gaussian component  $\mathcal{C}_G$  as follows

$$\mathcal{C} = \mathcal{C}_1 - \frac{1}{4\Phi}\mathcal{C}_1^2, \quad \text{with } \mathcal{C}_1 = \mathcal{C}_G \frac{dF}{d\mathcal{R}_G}, \quad (4)$$

where  $\Phi = \frac{2}{3}$  during radiation dominated period.  $\mathcal{C}_G$  is related to Gaussian primordial perturbation  $\mathcal{R}_G$  via

$$\mathcal{C}_G(r) = -2\Phi r \frac{d\mathcal{R}_G}{dr}. \quad (5)$$

The mass fraction  $\beta_k(M_{\text{PBH}})$  can be calculated as follows:

$$\beta_k(M_{\text{PBH}}) = \int_{\mathcal{D}} d\mathcal{C} \frac{M_{\text{PBH}}}{M_k} P_G(\mathcal{C}_G, \mathcal{R}_G) d\mathcal{C}_G d\mathcal{R}_G, \quad (6)$$

where  $\mathcal{D} = \{\mathcal{C}(\mathcal{C}_G, \mathcal{R}_G) > \mathcal{C}_{\text{th}} \wedge \mathcal{C}_1(\mathcal{C}_G, \mathcal{R}_G) < 2\Phi\}$ . The two-dimensional Gaussian distribution is

$$P_G(\mathcal{C}_G, \mathcal{R}_G) = \frac{1}{2\pi\sigma_c\sigma_r\sqrt{1-\gamma_{cr}^2}} \exp\left[-\frac{\mathcal{R}_G^2}{2\sigma_r^2} - \frac{1}{2(1-\gamma_{cr}^2)} \left(\frac{\mathcal{C}_G}{\sigma_c} - \frac{\gamma_{cr}\mathcal{R}_G}{\sigma_r}\right)^2\right]. \quad (7)$$

The correlators are given by

$$\sigma_c^2 = \frac{4\Phi^2}{9} \int_0^\infty \frac{dk}{k} (kr_m)^4 W^2(k, r_m) T^2(k, r_m) \mathcal{P}_{\mathcal{R}}(k), \quad (8)$$

$$\sigma_{cr}^2 = \frac{2\Phi}{3} \int_0^\infty \frac{dk}{k} (kr_m)^2 W(k, r_m) W_s(k, r_m) T^2(k, r_m) \mathcal{P}_{\mathcal{R}}(k), \quad (9)$$

$$\sigma_r^2 = \int_0^\infty \frac{dk}{k} W_s^2(k, r_m) T^2(k, r_m) \mathcal{P}_{\mathcal{R}}(k), \quad (10)$$

with  $\gamma_{cr} \equiv \frac{\sigma_{cr}^2}{\sigma_c\sigma_r}$  and  $r_m \simeq 2.4 \times 10^{-7} \text{Mpc} \left(\frac{g}{10.75}\right)^{1/12} \sqrt{\frac{M_H}{M_\odot}}$ . The top-hat window function  $W(k, r_m)$ , spherical-shell window function  $W_s(k, r_m)$  and the transfer function  $T(k, r_m)$  can be found in [68]. The PBH mass function can be obtained directly from the mass fraction:

$$\frac{df_{\text{PBH}}}{d\ln M_{\text{PBH}}} = \frac{1}{\Omega_{\text{DM}}} \int \frac{dM_k}{M_k} \beta_k(M_{\text{PBH}}) \left(\frac{M_{\text{eq}}}{M_k}\right)^{1/2}, \quad (11)$$

where  $M_{\text{eq}} \simeq 2.7 \times 10^{17} M_\odot$  is the horizon mass at radiation-matter equality and  $\Omega_{\text{DM}} = 0.12h^{-2}$  is the cold dark matter density. The PBH abundance  $f_{\text{PBH}} = \frac{\rho_{\text{PBH}}}{\rho_{\text{DM}}}\Big|_{\text{today}}$  can be expressed after integration:

$$f_{\text{PBH}} = \frac{1}{\Omega_{\text{DM}}} \int \frac{dM_{\text{PBH}}}{M_{\text{PBH}}} \int_{M_k^{\text{min}}} \frac{dM_k}{M_k} \left(\frac{M_{\text{eq}}}{M_k}\right)^{1/2} \left[1 - \frac{\mathcal{C}_{\text{th}}}{\Phi} - \frac{1}{\Phi} \left(\frac{M_{\text{PBH}}}{\mathcal{K}M_k}\right)^{1/\gamma}\right]^{-1/2} \\ \times \frac{\mathcal{K}}{\gamma} \left(\frac{M_{\text{PBH}}}{\mathcal{K}M_k}\right)^{\frac{1+\gamma}{\gamma}} \int d\mathcal{R}_G P_G(\mathcal{C}_G(M_{\text{PBH}}, \mathcal{R}_G), \mathcal{R}_G) \left(\frac{dF}{d\mathcal{R}_G}\right)^{-1}. \quad (12)$$

## B. $\mu$ -distortion calculation

For the  $\mu$ -distortion limits that constrain the amplitude of perturbations that form SMBHs, we employ the numerical techniques detailed in Refs. [60, 77, 78] to calculate the power spectrum amplitude that saturates the COBE-FIRAS  $\mu$ -type distortion limit. To be concentrate, it can be quantified by the dimensionless quantity  $\mu$  and calculated as follows:

$$\mu = \int dk \frac{k^2}{2\pi^2} P_{\mathcal{R}}(k) W_{\mu}(k) = \int \frac{dk}{k} \mathcal{P}_{\mathcal{R}}(k) W_{\mu}(k), \quad (13)$$

where  $P_{\mathcal{R}}(k)$  is the curvature power spectrum and  $\mathcal{P}_{\mathcal{R}}(k)$  is the dimensionless curvature power spectrum and they are related by

$$\mathcal{P}_{\mathcal{R}}(k) = \frac{k^3}{2\pi^2} P_{\mathcal{R}}(k). \quad (14)$$

$W_{\mu}(k)$  is the window function which contains details regarding the  $\mu$ -distortion. It can be numerically calculated by CLASS and we adopt the results from [60]:

$$W_{\mu}(k) = \exp \left[ \sum_{n=0}^6 z_n \ln^n \left( \frac{k}{1 \text{ Mpc}^{-1}} \right) \right], \quad (15)$$

with coefficients  $z_n$  provided in the Table 1 of [60]. We utilize the updated value of  $\mu < 4.7 \times 10^{-5}$  from Bianchini and Fabbian [79], which is a factor of 2 more stringent than the constraint originally reported by the COBE collaboration [33] and slightly tighter than the TRIS result [80].

## III. LOG-NORMAL POWER SPECTRUM CASE

A broad primordial power spectrum is more likely to arise in realistic inflation models. A commonly used broad power spectrum is the log-normal form given by [45, 69]

$$\mathcal{P}_{\mathcal{R}}(k) = \frac{A_{\text{LN}}}{\sqrt{2\pi}\Delta} \exp \left( -\frac{\ln^2(k/k_*)}{2\Delta^2} \right), \quad (16)$$

where  $A_{\text{LN}}$  is the amplitude,  $k_*$  is the peaked wavenumber and  $\Delta$  is the width. We recover the  $\delta$ -function spectrum

$$\mathcal{P}_{\mathcal{R}}(k) = A_{\text{LN}} k_* \delta(k - k_*) \quad (17)$$

for  $\Delta \rightarrow 0$ . Another form of the broad power spectrum, the broken power law, will be discussed in section IV. Then we show the impact of broadening on  $\mu$ -distortion under both Gaussian and non-Gaussian conditions.

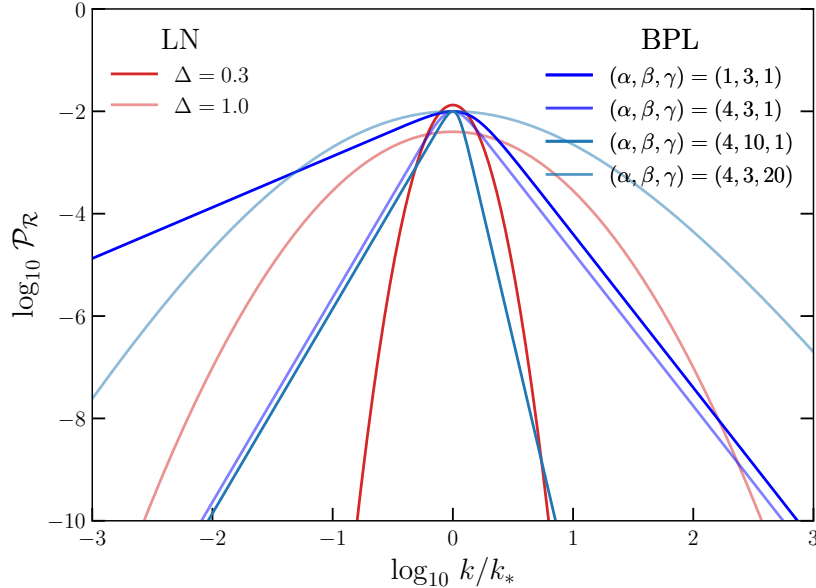


FIG. 1: The primordial broad power spectrum against the comoving-to-peak wavenumber ratio with log-normal (red, (16)) and broken power law (blue, (28)) form, where  $A_{\text{LN}} = A_{\text{BPL}} = 10^{-2}$ .

### A. Gaussian case

In the Gaussian case, the variance of the curvature is given by

$$A = \langle \mathcal{R}^2(\vec{x}) \rangle = \int_0^\infty \frac{dk}{k} \mathcal{P}_{\mathcal{R}}(k) = A_{\text{LN}}. \quad (18)$$

We note that the width  $\Delta$  does not affect the variance. Substituting (16) into (13) yields the  $\mu$ -distortion constraint on the variance of the curvature for the log-normal power spectrum, as shown by the solid lines in Figure 2. As a contrast, we also plot the constraints for the  $\delta$ -function power spectrum (17).

As the width of log-normal power spectrum  $\Delta$  is broader, the  $\mu$ -distortion constraints become increasingly stronger at large  $k$ . The reason is explained as follows. When  $k$  takes values between  $10$  and  $10^4 \text{ Mpc}^{-1}$ , the window function  $W_\mu$  is relatively large (due to the fact that the  $\mu$ -distortion primarily arises during this period). As the width of the power spectrum is broader, scales further away from  $k_*$  acquire greater amplitudes. Therefore, when  $k_* > 10^4 \text{ Mpc}^{-1}$ , the contribution of the power spectrum to the  $\mu$ -distortion increases according to (13), leading to a stricter constraint on  $A$ . Furthermore, the amplitude  $A$  required for  $f_{\text{PBH}} = 1$  slightly increases with the width. Then, the maximum PBH mass  $\mu$ -distortion required decreases which is smaller than  $10^4 M_\odot$ , in agreement with the as-

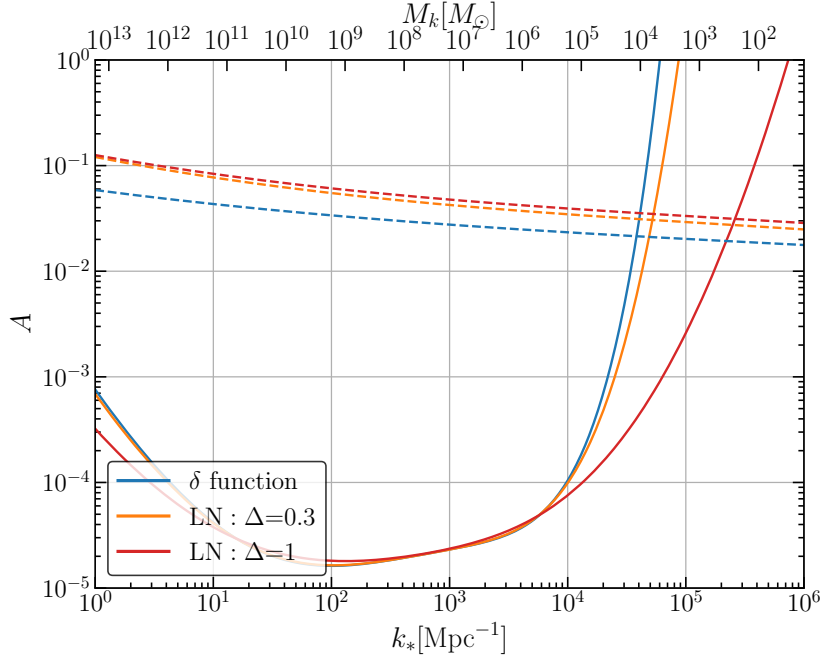


FIG. 2: The  $\mu$  constraints on the variance assuming Gaussian curvature perturbations for the  $\delta$ -function power spectrum (17) and log-normal power spectrum (16) respectively. The dashed lines show the corresponding PBH constraints (we choose  $f_{\text{PBH}} = 1$  constraints throughout the paper) on the variance calculated by (12). The upper x-axis shows the horizon mass in solar mass units (which is approximately the PBH mass) corresponding to each  $k_*$  value.

assumptions presented in the Refs.[45, 81].

## B. Non-Gaussian case

Non-Gaussianity has a significant impact on the properties of PBHs. Firstly, PBHs formed from non-Gaussian perturbations tends to cluster. Observational constraints on such clustering may limit the ability to circumvent  $\mu$ -distortion constraints for the generation of SMPBHs through large non-Gaussianity [82–85]. Secondly, there are stringent constraints on any non-Gaussian correlation between PBH-forming scales and CMB scales, through the restrictions imposed by photon-dark matter isocurvature perturbations [86–88]. More discussion can refer to [81].

Primordial local non-Gaussianity can be characterised by a Taylor expansion of comoving



curvature perturbation [64]

$$\mathcal{R}(\vec{x}) = \mathcal{R}_G(\vec{x}) + \tilde{f}_{\text{NL}} (\mathcal{R}_G^2(\vec{x}) - \langle \mathcal{R}_G^2(\vec{x}) \rangle) + \tilde{g}_{\text{NL}} \mathcal{R}_G^3(\vec{x}) + \dots, \quad (19)$$

where  $\tilde{f}_{\text{NL}} \equiv 3f_{\text{NL}}/5$  and  $\tilde{g}_{\text{NL}} \equiv 9g_{\text{NL}}/25$  are non-linearity parameters quantifying the magnitude of non-Gaussianity. Here, we focus only on the quadratic term and  $\tilde{f}_{\text{NL}} > 0$  because it corresponds to an improvement of the production of PBH and leave higher order terms for further research. Additionally, we assume that the Gaussian field  $\mathcal{R}_G$  has a log-normal form for its power spectrum, with a peak at  $k_*$  and amplitude  $A_G$ .

Then we examine two different types of non-Gaussianity. One is the perturbative non-Gaussianity, i.e. the linear term is predominant, specifically  $\tilde{f}_{\text{NL}}\sqrt{A_G} \ll 1$ . Another is non-perturbative non-Gaussianity, i.e. either  $\tilde{f}_{\text{NL}}$  or even higher-order terms dominate to such an extent that the power spectrum is entirely governed by these non-linear terms.

### 1. Perturbative non-Gaussian constraints

Here we present constraints in both the strictly perturbative limit of  $\tilde{f}_{\text{NL}}\sqrt{A_G} \ll 1$  and the borderline case of perturbativity  $\tilde{f}_{\text{NL}}\sqrt{A_G} = 1$ . Using the contraction that  $\langle \mathcal{R}_G^4 \rangle = 3\langle \mathcal{R}_G^2 \rangle^2 = 3A_G^2$ , (19) demonstrates that the total variance is given by

$$A \equiv \langle \mathcal{R}^2 \rangle = A_G + 2\tilde{f}_{\text{NL}}^2 A_G^2. \quad (20)$$

If we define  $\kappa$  as  $\tilde{f}_{\text{NL}}\sqrt{A_G}$ , then the variance can be expressed by

$$A = A_G(1 + 2\kappa^2). \quad (21)$$

To calculate  $\mu$ -distortion in the non-Gaussian case, we need to focus on the primordial power spectrum. As discussed in [89], corrections to this power spectrum arise from a single one-loop diagram, which leads to

$$P_{\mathcal{R}}(k) = P_{\mathcal{R}_G}(k) + \tilde{f}_{\text{NL}}^2 P_{\mathcal{R}_G^2}(k) = P_{\mathcal{R}_G}(k) + 2\tilde{f}_{\text{NL}}^2 \int \frac{d^3q}{(2\pi)^3} P_{\mathcal{R}_G}(q) P_{\mathcal{R}_G}(|\vec{k} - \vec{q}|). \quad (22)$$

Substituting (22) into (13), we obtain the spectral distortion

$$\mu = \int \frac{dk}{k} \mathcal{P}_{\mathcal{R}_G}(k) W_{\mu}(k) + \int \frac{dk}{k} \tilde{f}_{\text{NL}}^2 \mathcal{P}_{\mathcal{R}_G^2}(k) W_{\mu}(k). \quad (23)$$

To calculate  $\mathcal{P}_{\mathcal{R}_G^2}(k)$ , we use spherical coordinates as  $(q, \theta, \phi)$  assuming that  $\vec{k}$  points in  $z$  direction which leads to

$$\mathcal{P}_{\mathcal{R}_G^2}(k) = \int_{-1}^1 dy \int_0^\infty dq \frac{A_G^2}{\Delta^2} \frac{1}{2\pi} \frac{k^2}{q (\sqrt{k^2 - 2kqy + q^2})^3} \times \exp \left[ -\frac{1}{2\Delta^2} \left( \ln^2 \frac{q}{k_*} + \ln^2 \frac{\sqrt{k^2 - 2kqy + q^2}}{k_*} \right) \right]. \quad (24)$$

where  $y \equiv \cos\theta$ . We solve (24) numerically.

The method for determining the PBH abundance for arbitrary values of  $\tilde{f}_{\text{NL}}$  is described in [section II A](#). We note that non-Gaussianity would relax the PBH abundance constraints on the variance  $A$ . [Figure 3](#) illustrates the perturbative non-Gaussian scenarios for log-normal power spectrum with  $\Delta = 0.3$  compared with  $\delta$  function case. We find that, under strict perturbative conditions, the  $\mu$ -distortion nearly coincides with the Gaussian case with broadening power spectrum. Examining the case at the perturbation boundary, we find that broadening weakens the  $\mu$ -distortion constraints. However, due to the difference in abundance constraints on  $A$ , the maximum PBH mass in the  $\delta$  function case is still larger.

## 2. Non-perturbative case : $\chi^2$ distribution

In this case, the comoving curvature perturbation can be expressed in the following form in terms of its Gaussian component

$$\mathcal{R}(\vec{x}) = \mathcal{R}_G^2(\vec{x}) - \langle \mathcal{R}_G^2(\vec{x}) \rangle. \quad (25)$$

Then the variance can be given by

$$A \equiv \int_0^\infty \frac{dk}{k} \mathcal{P}_{\mathcal{R}_G^2}(k) = 2A_G^2. \quad (26)$$

The  $\mu$ -distortion can then be computed using (13) with  $\mathcal{P}_{\mathcal{R}}(k)$  substituted with (24). The result can be put in the form

$$\mu = \int \frac{dk}{k} \mathcal{P}_{\mathcal{R}_G^2}(k) W_\mu(k). \quad (27)$$

[Figure 4](#) illustrate the  $\chi^2$  non-Gaussian scenario compared with Gaussian scenario for different width  $\Delta$ . It is clear that as the width of the power spectrum broadens, the  $\mu$ -distortion constraint in the Gaussian case gradually strengthens in the large  $k$  region. In contrast, the

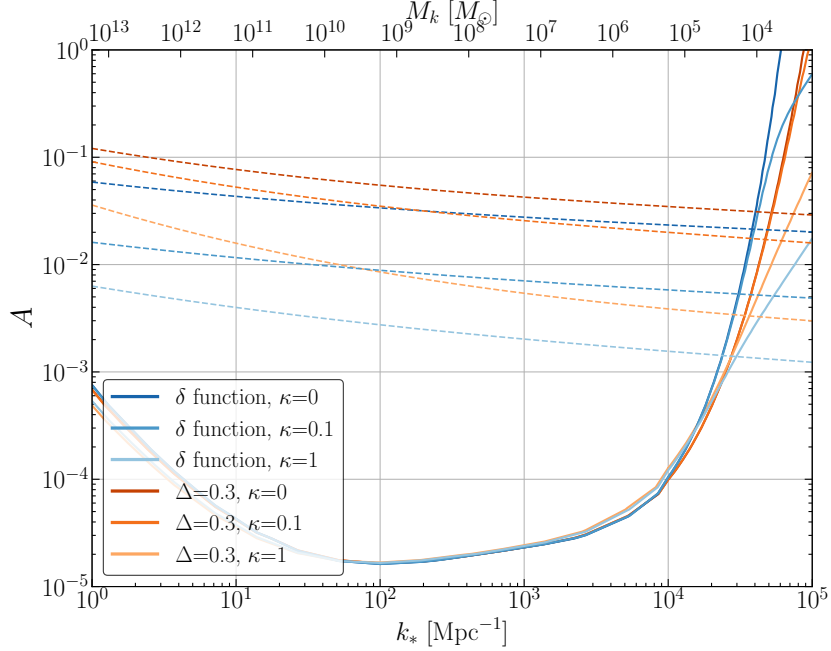


FIG. 3: Constraints on the variance assuming perturbative non-Gaussian curvature perturbations, assuming log-normal power spectrum (16) with  $\Delta = 0.3$  and  $\delta$ -function power spectrum (17) respectively. The solid lines represent the  $\mu$ -distortion constraints, while the dashed lines represent the abundance constraints requiring  $f_{\text{PBH}} = 1$ . Here,  $\kappa$  is defined as  $\tilde{f}_{\text{NL}}\sqrt{A_{\text{G}}}$  and quantifies the relative non-Gaussian contribution to the total variance.

$\mu$ -distortion constraint in the non-Gaussian case exhibits a slight decrease followed by an increase. This results in the non-Gaussian case having a stronger constraint in the large  $k$  region than Gaussian case when the power spectrum width is small, but a weaker constraint when the width is larger.

We can explain this result by considering the effect of power spectrum width  $\Delta$  on  $\mathcal{P}_{\mathcal{R}_{\text{G}}}(k)$  (16) and  $\mathcal{P}_{\mathcal{R}_{\text{G}}^2}(k)$  (24). When the width  $\Delta$  is small,  $\frac{1}{k}\mathcal{P}_{\mathcal{R}_{\text{G}}^2}(k)$  is larger than  $\frac{1}{k}\mathcal{P}_{\mathcal{R}_{\text{G}}}(k)$  in the region below  $k_*$ , which results in a greater contribution to the  $\mu$ -distortion and stronger constraint on the variance  $A$  when  $k_* \gtrsim 10^4 \text{Mpc}^{-1}$ . However, as the width  $\Delta$  broadens, this relationship reverses. In the above discussion, we have considered the impact of the  $\chi^2$  distribution on the variance  $A$ .

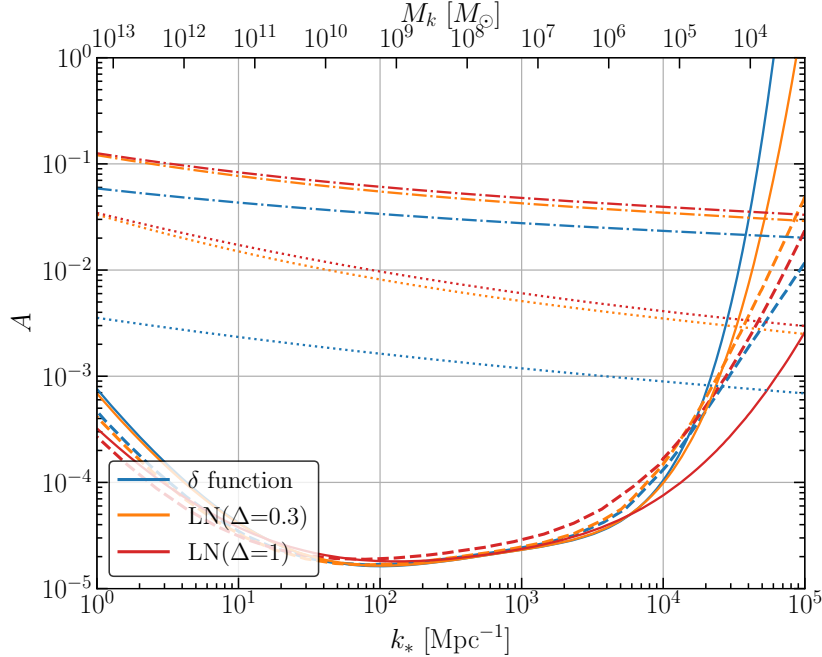


FIG. 4: Constraints on the variance for Gaussian (solid) and  $\chi^2$  (dashed) statistics for  $\delta$ -function (17) and LN (16) power spectrum with different  $\Delta$ . The horizontal dash-dotted line and dotted line represent the  $f_{\text{PBH}} = 1$  constraints for PBHs in the Gaussian and  $\chi^2$  cases, respectively.

#### IV. BROKEN POWER LAW POWER SPECTRUM CASE

The broken power law (BPL) form of power spectrum is defined as

$$\mathcal{P}_{\mathcal{R}}(k) = A_{\text{BPL}} \frac{(\alpha + \beta)^\gamma}{[\beta(k/k_*)^{-\alpha/\gamma} + \alpha(k/k_*)^{\beta/\gamma}]^\gamma} \quad (28)$$

where  $\alpha$  describes the growth,  $\beta$  describes the decay and  $\gamma$  the width of the spectrum at the scale  $k_*$ . This parametrisation can describe a common class of spectra that exhibit peaks, often associated with single-field inflation or curvaton models, with typical values for  $\alpha$  being  $0 < \alpha \lesssim 4$ . Additionally, in quasi-inflection-point models that give rise to stellar-mass PBHs, one typically expects  $\beta \gtrsim 0.5$ , while for curvaton models  $\beta \gtrsim 2$ .

To generate the parameter space constraint plots for the BPL equivalent to the log-normal case, we fixed two of the parameters  $(\alpha, \beta, \gamma)$ . The fixed values were identified  $(\alpha, \beta, \gamma) = (4, 3, 1)$  [46, 90]. The parameter choices for comparison can be seen in Figure 1. It is important to emphasize that the width of the BPL power spectrum broadens as  $\alpha$  decreases,  $\beta$  decreases, or  $\gamma$  increases. The procedure for calculating the  $\mu$ -distortion and PBH abundance using the BPL power spectrum in (non-)Gaussian case is similar to that

for the log-normal case, see [section II](#).

### A. Gaussian case

The variance now is given by

$$A = \langle \mathcal{R}^2(\vec{x}) \rangle = \int \frac{dk}{k} \mathcal{P}_{\mathcal{R}}(k) = A_{\text{BPL}} \int \frac{dk}{k} \frac{(\alpha + \beta)^\gamma}{[\beta(k/k_*)^{-\alpha/\gamma} + \alpha(k/k_*)^{\beta/\gamma}]^\gamma}. \quad (29)$$

The expression above cannot be solved analytically. We emphasize that, in contrast to the log-normal case, the variance  $A$  depends on the parameters  $\alpha$ ,  $\beta$  and  $\gamma$  of the BPL power spectrum besides the amplitude.

The constraints of different parameter combinations on  $\mu$ -distortion and PBH abundance are summarized in [Figure 5](#). We can observe that when the broadening of the BPL power spectrum undergoes significant changes, the  $\mu$ -distortion constraints show noticeable variations. Moreover, the broader the spectrum, the stronger the constraints in the high- $k_*$  region, while in the low- $k_*$  region, the constraints are similar to those in the log-normal case. In contrast to the log-normal case, the changes in abundance constraints due to different parameter combinations are minimal. In summary, the broader the spectrum, the smaller the allowed maximum PBH mass.

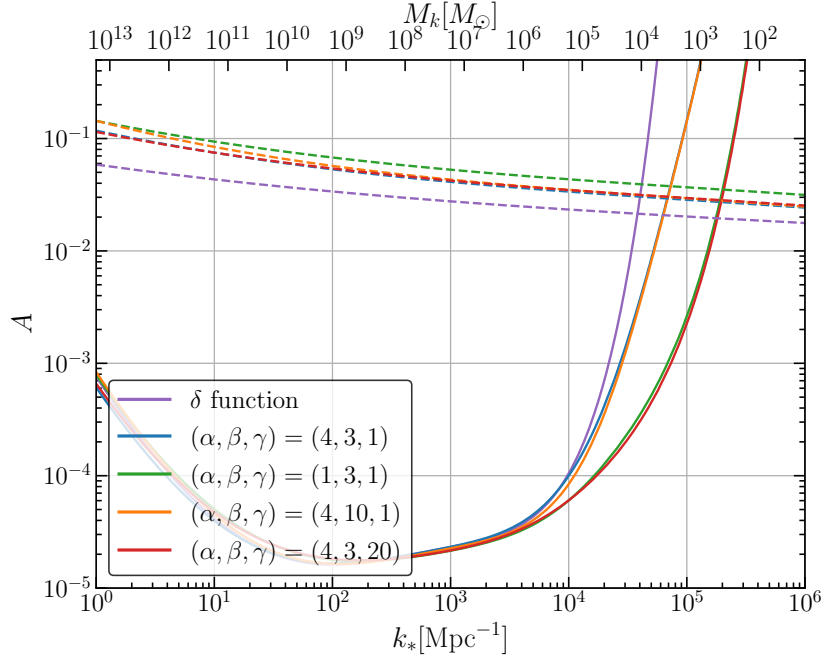


FIG. 5: Constraints on the variance assuming Gaussian curvature perturbations for BPL (28) compared with  $\delta$ -function (17) power spectrum. We can see that only when the width of the BPL power spectrum undergo a significant change, the  $\mu$ -constraints show noticeable variations in the high- $k_*$  region .

## B. Non-Gaussian case

### 1. Perturbative non-Gaussian constraints

Similar to the log-normal case, we first need to calculate  $P_{\mathcal{R}_G^2}(k)$ . However, the result now is more complex:

$$\begin{aligned}
P_{\mathcal{R}_G^2}(k) &= 2 \int \frac{d^3q}{(2\pi)^3} P_{\mathcal{R}_G}(q) P_{\mathcal{R}_G}(|\vec{k} - \vec{q}|) \\
&= 2 \int \frac{d^3q}{(2\pi)^3} \frac{2\pi^2}{q^3} A_{\text{BPL}} \frac{(\alpha + \beta)^\gamma}{\left[ \beta \left( \frac{q}{k_*} \right)^{-\frac{\alpha}{\gamma}} + \alpha \left( \frac{q}{k_*} \right)^{\frac{\beta}{\gamma}} \right]^\gamma} |\vec{k} - \vec{q}|^3 A_{\text{BPL}} \frac{(\alpha + \beta)^\gamma}{\left[ \beta \left( \frac{|\vec{k} - \vec{q}|}{k_*} \right)^{-\frac{\alpha}{\gamma}} + \alpha \left( \frac{|\vec{k} - \vec{q}|}{k_*} \right)^{\frac{\beta}{\gamma}} \right]^\gamma} \\
&= 2 \int_0^\infty dq \int_{-1}^1 dy \pi^2 \frac{A_{\text{BPL}}^2}{q} \frac{1}{(\sqrt{k^2 - 2kqy + q^2})^3} \frac{(\alpha + \beta)^\gamma}{\left[ \beta \left( \frac{q}{k_*} \right)^{-\frac{\alpha}{\gamma}} + \alpha \left( \frac{q}{k_*} \right)^{\frac{\beta}{\gamma}} \right]^\gamma} \\
&\quad \times \frac{(\alpha + \beta)^\gamma}{\left[ \beta \left( \frac{\sqrt{k^2 - 2kqy + q^2}}{k_*} \right)^{-\frac{\alpha}{\gamma}} + \alpha \left( \frac{\sqrt{k^2 - 2kqy + q^2}}{k_*} \right)^{\frac{\beta}{\gamma}} \right]^\gamma}. \tag{30}
\end{aligned}$$

The result definitely cannot be solved analytically. [Figure 6](#) illustrates the perturbative non-Gaussian scenarios for the cases  $(\alpha, \beta, \gamma) = (4, 3, 20)$  and  $(4, 10, 1)$ . In the perturbative non-Gaussian region, the  $\mu$ -distortion constraints for case  $(4, 3, 20)$  are always stronger than those for case  $(4, 10, 1)$ .

### 2. Non-perturbative case: $\chi^2$ distribution

To obtain the constraints in the  $\chi^2$  case, we follow a procedure similar to the log-normal scenario. By substituting [\(30\)](#) and [\(14\)](#) into [\(13\)](#) and using [\(29\)](#), we obtain [Figure 7](#).

The commonality among these two parameter combinations is that the  $\mu$ -distortion constraints in the  $\chi^2$  case are not significantly different from those in the Gaussian case. Due to the impact of non-Gaussianity on the PBH abundance calculation, considering the  $\chi^2$  non-Gaussian form, the allowed maximum PBH mass is increased by less than an order of magnitude compared to the Gaussian case. However, the specific value remains below  $10^5 M_\odot$ .

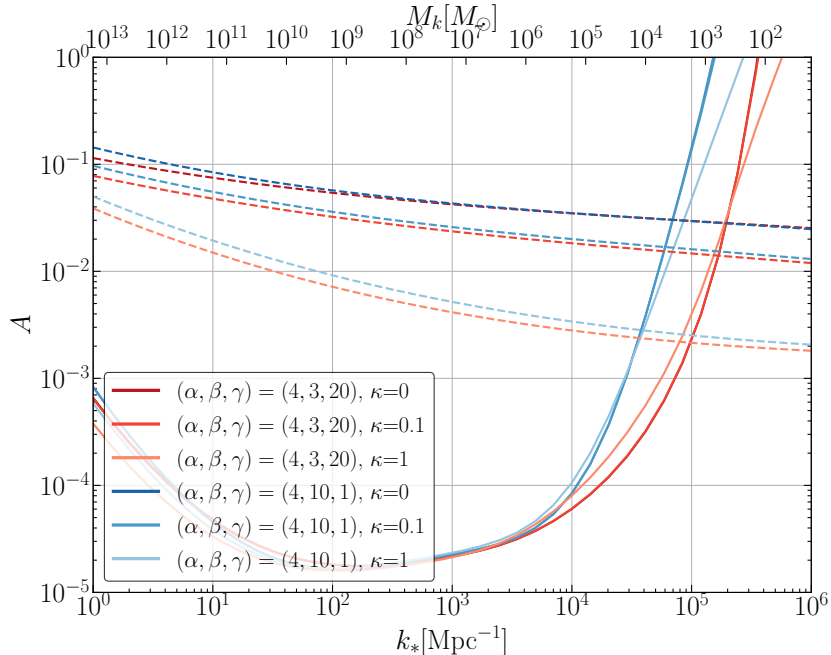


FIG. 6: The solid (dashed) lines represent the  $\mu$ -distortion ( $f_{\text{PBH}} = 1$  abundance) constraints on the variance.  $\kappa$  is defined as  $\tilde{f}_{\text{NL}}\sqrt{A_{\text{G}}}$  and quantifies the relative non-Gaussian contribution to the total variance. We note that the  $\mu$ -distortion constraints in the Gaussian case nearly coincide with those for  $\kappa = 0.1$ .

## V. CONCLUSIONS

In recent years,  $\mu$ -distortion constraints have been widely applied to probe the viability of SMPBHs originating in the early universe. Prior studies have established  $\mu$ -distortion as a stringent observational limit on the primordial power spectrum and introduce non-Gaussianity to evade or relax the constraint. However, these studies largely assumed  $\delta$ -function power spectrum (17) and do not capture the effects of a more realistic power spectrum with certain width. Our study addresses this gap by investigating  $\mu$ -distortion constraints for broad power spectrum models, specifically log-normal (16) and broken power law (28) distributions, both of which reflect potential early-universe scenarios more accurately than single-peaked models.

For the log-normal case, when the width is small ( $\Delta \lesssim 0.3$ ), the situation is essentially the same as the monochromatic case, as expected [45, 81]. However, as the width is broader, the effects of the width and non-Gaussianity on the distortion constraints do not simply



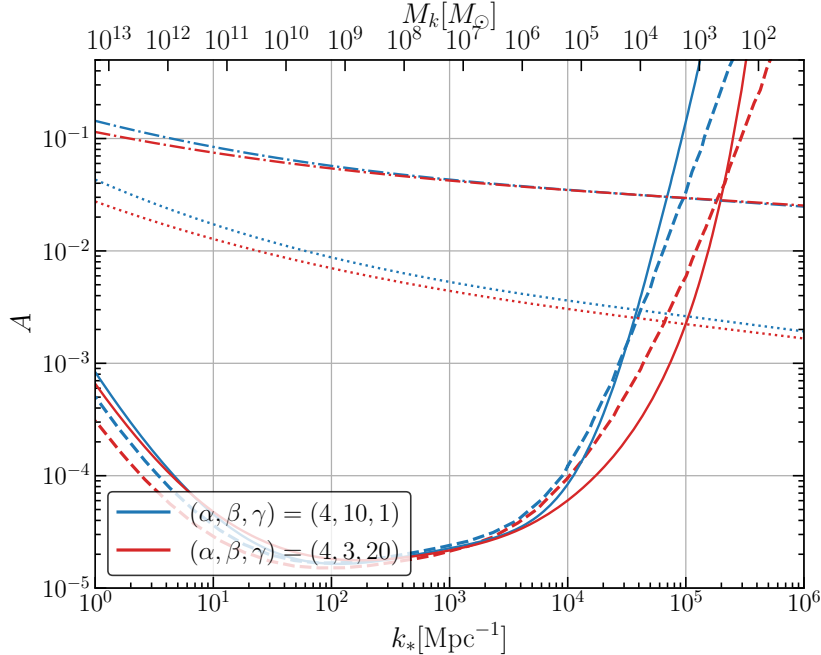


FIG. 7: Constraints on the variance for Gaussian (solid) and  $\chi^2$  (dashed) statistics for different  $(\alpha, \beta, \gamma)$ . The horizontal dash-dotted line and dotted line represent the  $f_{\text{PBH}} = 1$  constraints for PBHs in the Gaussian and  $\chi^2$  cases, respectively.

add together, when the width reaches a certain threshold, the non-Gaussian constraints may even become weaker than those in the Gaussian case in the large  $k$  space. For the BPL power spectrum, the  $\mu$ -distortion constraints in the small  $k$  space is similar to log-normal and  $\delta$ -function case, regardless of the existence of non-Gaussianity. The broadening of the power spectrum is positively correlated with the  $\mu$ -distortion constraints in the high- $k_*$  region, while non-Gaussianity enhances the constraints in the case of narrow broadening and weakens them in the case of wide broadening, the same as log-normal case.

For both broad power spectrum above, we found that  $\mu$ -distortion limits restrict the maximum PBH mass to approximately  $10^4 M_\odot$ , suggesting that PBHs with masses sufficient to seed SMBHs (i.e.  $\gtrsim 10^6 M_\odot$ ) cannot form under the current constraints (see Table I for the summary). However, if higher-order non-Gaussianity is considered as suggested in [81], we expect the horizontal line representing the PBH abundance to bypass the  $\mu$ -distortion constraints at the bottom in the  $k_*$ -range from  $10^2$  to  $10^4 \text{ Mpc}^{-1}$ . Our analysis shows that the  $\mu$ -distortion constraints in this region on the variance are independent of both the broadening of the power spectrum and the existence of non-Gaussianity. Therefore,

generating SMPBHs may require higher-order non-Gaussianity to relax the variance for the abundance of the corresponding PBHs, a possibility that warrants further investigation.

## Acknowledgments

This work is supported by National Key Research and Development Program of China (Grant No. 2021YFC2203004), NSFC (Grant No.12075246), and the Fundamental Research Funds for the Central Universities.

- 
- [1] S. Hawking, *Gravitationally collapsed objects of very low mass*, *Mon. Not. Roy. Astron. Soc.* **152** (1971) 75.
  - [2] B. J. Carr and S. W. Hawking, *Black holes in the early Universe*, *Mon. Not. Roy. Astron. Soc.* **168** (1974) 399–415.
  - [3] Y. B. Zel’dovich and I. D. Novikov, *The Hypothesis of Cores Retarded during Expansion and the Hot Cosmological Model*, *Soviet Astron. AJ (Engl. Transl. )*, **10** (1967) 602.
  - [4] B. Carr, F. Kühnel, and M. Sandstad, *Primordial black holes as dark matter*, *Phys. Rev. D* **94** (Oct, 2016) 083504.
  - [5] G. F. Chapline, *Cosmological effects of primordial black holes*, *Nature* **253** (1975), no. 5489 251–252.
  - [6] P. Meszaros, *Primeval black holes and galaxy formation*, *Astron. Astrophys.* **38** (1975) 5–13.
  - [7] B. Carr, K. Kohri, Y. Sendouda, and J. Yokoyama, *Constraints on primordial black holes*, *Rept. Prog. Phys.* **84** (2021), no. 11 116902, [[arXiv:2002.12778](#)].
  - [8] M. Calzà, D. Pedrotti, and S. Vagnozzi, *Primordial regular black holes as all the dark matter. I. Time-radial-symmetric metrics*, *Phys. Rev. D* **111** (2025), no. 2 024009, [[arXiv:2409.02804](#)].
  - [9] M. Calzà, D. Pedrotti, and S. Vagnozzi, *Primordial regular black holes as all the dark matter. II. Non-time-radial-symmetric and loop quantum gravity-inspired metrics*, *Phys. Rev. D* **111** (2025), no. 2 024010, [[arXiv:2409.02807](#)].
  - [10] B. Carr, S. Clesse, J. Garcia-Bellido, M. Hawkins, and F. Kuhnel, *Observational evidence for primordial black holes: A positivist perspective*, *Phys. Rept.* **1054** (2024) 1–68,

- [arXiv:2306.03903].
- [11] T. Nakama, T. Suyama, and J. Yokoyama, *Supermassive black holes formed by direct collapse of inflationary perturbations*, *Phys. Rev. D* **94** (2016), no. 10 103522, [arXiv:1609.02245].
  - [12] B. Carr, F. Kuhnel, and M. Sandstad, *Primordial Black Holes as Dark Matter*, *Phys. Rev. D* **94** (2016), no. 8 083504, [arXiv:1607.06077].
  - [13] J. García-Bellido, *Massive Primordial Black Holes as Dark Matter and their detection with Gravitational Waves*, *J. Phys. Conf. Ser.* **840** (2017), no. 1 012032, [arXiv:1702.08275].
  - [14] M. Sasaki, T. Suyama, T. Tanaka, and S. Yokoyama, *Primordial black holes—perspectives in gravitational wave astronomy*, *Classical and Quantum Gravity* **35** (feb, 2018) 063001.
  - [15] B. Carr and F. Kühnel, *Primordial black holes as dark matter: Recent developments*, *Annual Review of Nuclear and Particle Science* **70** (2020), no. Volume 70, 2020 355–394.
  - [16] B. Carr and F. Kuhnel, *Primordial black holes as dark matter candidates*, *SciPost Phys. Lect. Notes* **48** (2022) 1, [arXiv:2110.02821].
  - [17] A. M. Green and B. J. Kavanagh, *Primordial black holes as a dark matter candidate*, *Journal of Physics G: Nuclear and Particle Physics* **48** (feb, 2021) 043001.
  - [18] A. Escrivà, F. Kuhnel, and Y. Tada, *Primordial Black Holes*, *arXiv e-prints* (Nov., 2022) arXiv:2211.05767, [arXiv:2211.05767].
  - [19] S. Pi, *Non-Gaussianities in primordial black hole formation and induced gravitational waves*, *arXiv e-prints* (Apr., 2024) arXiv:2404.06151, [arXiv:2404.06151].
  - [20] G. Domènech and M. Sasaki, *Probing primordial black hole scenarios with terrestrial gravitational wave detectors*, *Classical and Quantum Gravity* **41** (jun, 2024) 143001.
  - [21] M. Y. Khlopov, *Primordial Black Holes*, *Res. Astron. Astrophys.* **10** (2010) 495–528, [arXiv:0801.0116].
  - [22] H.-L. Huang, Y. Cai, J.-Q. Jiang, J. Zhang, and Y.-S. Piao, *Supermassive Primordial Black Holes for Nano-Hertz Gravitational Waves and High-redshift JWST Galaxies*, *Res. Astron. Astrophys.* **24** (2024), no. 9 091001, [arXiv:2306.17577].
  - [23] H.-L. Huang and Y.-S. Piao, *Toward supermassive primordial black holes from inflationary bubbles*, *Phys. Rev. D* **110** (2024), no. 2 023501, [arXiv:2312.11982].
  - [24] D. Hooper, A. Ireland, G. Krnjaic, and A. Stebbins, *Supermassive primordial black holes from inflation*, *JCAP* **04** (2024) 021, [arXiv:2308.00756].
  - [25] Y. Gouttenoire, S. Trifinopoulos, G. Valogiannis, and M. Vanvlasselaer, *Scrutinizing the*

- primordial black hole interpretation of PTA gravitational waves and JWST early galaxies*, *Phys. Rev. D* **109** (2024), no. 12 123002, [[arXiv:2307.01457](#)].
- [26] P. F. Depta, K. Schmidt-Hoberg, P. Schwaller, and C. Tasillo, *Do pulsar timing arrays observe merging primordial black holes?*, [arXiv:2306.17836](#).
- [27] A. Guo, J. Zhang, and H. Yang, *Superradiant clouds may be relevant for close compact object binaries*, *Phys. Rev. D* **110** (2024), no. 2 023022, [[arXiv:2401.15003](#)].
- [28] M. Volonteri, M. Habouzit, and M. Colpi, *The origins of massive black holes*, *Nature Rev. Phys.* **3** (2021), no. 11 732–743, [[arXiv:2110.10175](#)].
- [29] P. Dayal, *Exploring a primordial solution for early black holes detected with the JWST*, *Astron. Astrophys.* **690** (2024) A182, [[arXiv:2407.07162](#)].
- [30] H.-L. Huang, Y.-T. Wang, and Y.-S. Piao, *Supermassive primordial black holes for the GHZ9 and UHZ1 observed by the JWST*, [arXiv:2410.05891](#).
- [31] H.-L. Huang, J.-Q. Jiang, J. He, Y.-T. Wang, and Y.-S. Piao, *Sub-Eddington accreting supermassive primordial black holes explain Little Red Dots*, [arXiv:2410.20663](#).
- [32] H.-L. Huang, J.-Q. Jiang, and Y.-S. Piao, *High-redshift JWST massive galaxies and the initial clustering of supermassive primordial black holes*, *Phys. Rev. D* **110** (2024), no. 10 103540, [[arXiv:2407.15781](#)].
- [33] D. J. Fixsen, E. S. Cheng, J. M. Gales, J. C. Mather, R. A. Shafer, and E. L. Wright, *The Cosmic Microwave Background spectrum from the full COBE FIRAS data set*, *Astrophys. J.* **473** (1996) 576, [[astro-ph/9605054](#)].
- [34] J. C. Mather et al., *Measurement of the Cosmic Microwave Background spectrum by the COBE FIRAS instrument*, *Astrophys. J.* **420** (1994) 439–444.
- [35] J. C. Mather et al., *A Preliminary measurement of the Cosmic Microwave Background spectrum by the Cosmic Background Explorer (COBE) satellite*, *Astrophys. J. Lett.* **354** (1990) L37–L40.
- [36] Y. B. Zeldovich and R. A. Sunyaev, *The Interaction of Matter and Radiation in a Hot-Model Universe*, *Astrophys. Space Sci.* **4** (1969) 301–316.
- [37] J. Chluba and R. A. Sunyaev, *The evolution of CMB spectral distortions in the early Universe*, *Mon. Not. Roy. Astron. Soc.* **419** (2012) 1294–1314, [[arXiv:1109.6552](#)].
- [38] A. Illarionov and R. Siuniaevev, *Comptonization, characteristic radiation spectra, and thermal balance of low-density plasma*, *Soviet Astronomy*, vol. 18, Jan.-Feb. 1975, p. 413–419.

- Translation. Astronomicheskii Zhurnal, vol. 51, July-Aug. 1974, p. 698-711. 18 (1975) 413-419.*
- [39] R. Sunyaev and Y. B. Zeldovich, *The interaction of matter and radiation in the hot model of the universe, ii, Astrophysics and Space Science* **7** (1970) 20–30.
- [40] J. Chluba, *Which spectral distortions does  $\Lambda$ CDM actually predict?*, *Mon. Not. Roy. Astron. Soc.* **460** (2016), no. 1 227–239, [[arXiv:1603.02496](#)].
- [41] G. De Zotti, M. Negrello, G. Castex, A. Lapi, and M. Bonato, *Another look at distortions of the Cosmic Microwave Background spectrum*, *JCAP* **03** (2016) 047, [[arXiv:1512.04816](#)].
- [42] R. Sunyaev and Y. B. Zeldovich, *The observations of relic radiation as a test of the nature of x-ray radiation from the clusters of galaxies*, *Comments on Astrophysics and Space Physics, Vol. 4, p. 173* **4** (1972) 173.
- [43] M. Birkinshaw, *The Sunyaev-Zel'dovich effect*, *Phys. Rept.* **310** (1999) 97–195, [[astro-ph/9808050](#)].
- [44] K. Kohri, T. Nakama, and T. Suyama, *Testing scenarios of primordial black holes being the seeds of supermassive black holes by ultracompact minihalos and CMB  $\mu$ -distortions*, *Phys. Rev. D* **90** (2014), no. 8 083514, [[arXiv:1405.5999](#)].
- [45] A. D. Gow, C. T. Byrnes, P. S. Cole, and S. Young, *The power spectrum on small scales: Robust constraints and comparing PBH methodologies*, *JCAP* **02** (2021) 002, [[arXiv:2008.03289](#)].
- [46] X. Pritchard and C. T. Byrnes, *Constraining the impact of standard model phase transitions on primordial black holes*, [arXiv:2407.16563](#).
- [47] K. Kasai, M. Kawasaki, K. Murai, and S. Neda, *Supermassive black hole formation from Affleck-Dine mechanism with suppressed clustering on large scales*, [arXiv:2405.09790](#).
- [48] W.-Y. Ai, L. Heurtier, and T. H. Jung, *Primordial black holes from an interrupted phase transition*, [arXiv:2409.02175](#).
- [49] P.-X. Lin and Y.-S. Piao, *Populating the landscape in an inhomogeneous universe*, *Phys. Rev. D* **105** (2022), no. 6 063534, [[arXiv:2111.09174](#)].
- [50] P.-X. Lin, H.-L. Huang, J. Zhang, and Y.-S. Piao, *On primordial universe in anti-de Sitter landscape*, *Phys. Lett. B* **855** (2024) 138768, [[arXiv:2211.05265](#)].
- [51] H.-H. Li, G. Ye, and Y.-S. Piao, *Is the NANOGraw signal a hint of  $dS$  decay during inflation?*, *Phys. Lett. B* **816** (2021) 136211, [[arXiv:2009.14663](#)].

- [52] G. Ye and Y.-S. Piao, *Is the Hubble tension a hint of AdS phase around recombination?*, *Phys. Rev. D* **101** (2020), no. 8 083507, [[arXiv:2001.02451](#)].
- [53] J.-Q. Jiang and Y.-S. Piao, *Testing AdS early dark energy with Planck, SPTpol, and LSS data*, *Phys. Rev. D* **104** (2021), no. 10 103524, [[arXiv:2107.07128](#)].
- [54] G. Ye, J. Zhang, and Y.-S. Piao, *Alleviating both  $H_0$  and  $S_8$  tensions: Early dark energy lifts the CMB-lockdown on ultralight axion*, *Phys. Lett. B* **839** (2023) 137770, [[arXiv:2107.13391](#)].
- [55] H. Wang and Y.-S. Piao, *Dark energy in light of recent DESI BAO and Hubble tension*, [arXiv:2404.18579](#).
- [56] H. Wang, Z.-Y. Peng, and Y.-S. Piao, *Can recent DESI BAO measurements accommodate a negative cosmological constant?*, [arXiv:2406.03395](#).
- [57] T. Nakama, B. Carr, and J. Silk, *Limits on primordial black holes from  $\mu$  distortions in cosmic microwave background*, *Phys. Rev. D* **97** (2018), no. 4 043525, [[arXiv:1710.06945](#)].
- [58] C. Ünal, E. D. Kovetz, and S. P. Patil, *Multimessenger probes of inflationary fluctuations and primordial black holes*, *Phys. Rev. D* **103** (2021), no. 6 063519, [[arXiv:2008.11184](#)].
- [59] A. D. Gow, H. Assadullahi, J. H. P. Jackson, K. Koyama, V. Vennin, and D. Wands, *Non-perturbative non-Gaussianity and primordial black holes*, *EPL* **142** (2023), no. 4 49001, [[arXiv:2211.08348](#)].
- [60] D. Sharma, J. Lesgourgues, and C. T. Byrnes, *Spectral distortions from acoustic dissipation with non-Gaussian (or not) perturbations*, *JCAP* **07** (2024) 090, [[arXiv:2404.18474](#)].
- [61] Y. Cai, M. Zhu, and Y.-S. Piao, *Primordial Black Holes from Null Energy Condition Violation during Inflation*, *Phys. Rev. Lett.* **133** (2024), no. 2 021001, [[arXiv:2305.10933](#)].
- [62] S. Balaji, S. Ando, M. Fairbairn, N. Hiroshima, and K. Ishiwata, *Supermassive black holes from inflation constrained by dark matter substructure*, [arXiv:2408.11098](#).
- [63] C. T. Byrnes, E. J. Copeland, and A. M. Green, *Primordial black holes as a tool for constraining non-Gaussianity*, *Phys. Rev. D* **86** (2012) 043512, [[arXiv:1206.4188](#)].
- [64] S. Young and C. T. Byrnes, *Primordial black holes in non-Gaussian regimes*, *JCAP* **08** (2013) 052, [[arXiv:1307.4995](#)].
- [65] G. Franciolini, A. Kehagias, S. Matarrese, and A. Riotto, *Primordial Black Holes from Inflation and non-Gaussianity*, *JCAP* **03** (2018) 016, [[arXiv:1801.09415](#)].
- [66] H.-L. Huang, J.-Q. Jiang, and Y.-S. Piao, *High-redshift JWST massive galaxies and the*

- initial clustering of supermassive primordial black holes*, [arXiv:2407.15781](#).
- [67] Q.-Y. Lan and Y.-S. Piao, *Prepare inflationary universe via the Euclidean charged wormhole*, [arXiv:2411.13844](#).
- [68] S. Young, *Peaks and primordial black holes: the effect of non-Gaussianity*, *JCAP* **05** (2022), no. 05 037, [[arXiv:2201.13345](#)].
- [69] G. Ferrante, G. Franciolini, A. Iovino, Junior., and A. Urbano, *Primordial non-Gaussianity up to all orders: Theoretical aspects and implications for primordial black hole models*, *Phys. Rev. D* **107** (2023), no. 4 043520, [[arXiv:2211.01728](#)].
- [70] I. Musco, *Threshold for primordial black holes: Dependence on the shape of the cosmological perturbations*, *Phys. Rev. D* **100** (2019), no. 12 123524, [[arXiv:1809.02127](#)].
- [71] S. Young, *The primordial black hole formation criterion re-examined: Parametrisation, timing and the choice of window function*, *Int. J. Mod. Phys. D* **29** (2019), no. 02 2030002, [[arXiv:1905.01230](#)].
- [72] S. Young, I. Musco, and C. T. Byrnes, *Primordial black hole formation and abundance: contribution from the non-linear relation between the density and curvature perturbation*, *JCAP* **11** (2019) 012, [[arXiv:1904.00984](#)].
- [73] I. Musco, J. C. Miller, and A. G. Polnarev, *Primordial black hole formation in the radiative era: Investigation of the critical nature of the collapse*, *Class. Quant. Grav.* **26** (2009) 235001, [[arXiv:0811.1452](#)].
- [74] I. Musco and J. C. Miller, *Primordial black hole formation in the early universe: critical behaviour and self-similarity*, *Class. Quant. Grav.* **30** (2013) 145009, [[arXiv:1201.2379](#)].
- [75] I. Musco, V. De Luca, G. Franciolini, and A. Riotto, *Threshold for primordial black holes. II. A simple analytic prescription*, *Phys. Rev. D* **103** (2021), no. 6 063538, [[arXiv:2011.03014](#)].
- [76] A. J. Iovino, G. Perna, A. Riotto, and H. Veermäe, *Curbing PBHs with PTAs*, *JCAP* **10** (2024) 050, [[arXiv:2406.20089](#)].
- [77] B. Cyr, T. Kite, J. Chluba, J. C. Hill, D. Jeong, S. K. Acharya, B. Bolliet, and S. P. Patil, *Disentangling the primordial nature of stochastic gravitational wave backgrounds with CMB spectral distortions*, [arXiv:2309.02366](#).
- [78] M. Tagliacuzzi, M. Braglia, F. Finelli, and M. Pieroni, *The quest of CMB spectral distortions to probe the scalar-induced gravitational wave background interpretation in PTA data*, [arXiv:2310.08527](#).

- [79] F. Bianchini and G. Fabbian, *CMB spectral distortions revisited: A new take on  $\mu$  distortions and primordial non-Gaussianities from FIRAS data*, *Phys. Rev. D* **106** (2022), no. 6 063527, [[arXiv:2206.02762](#)].
- [80] M. Gervasi, M. Zannoni, A. Tartari, G. Boella, and G. Sironi, *TRIS II: search for CMB spectral distortions at 0.60, 0.82 and 2.5 GHz*, *Astrophys. J.* **688** (2008) 24, [[arXiv:0807.4750](#)].
- [81] C. T. Byrnes, J. Lesgourgues, and D. Sharma, *Robust  $\mu$ -distortion constraints on primordial supermassive black holes from non-Gaussian perturbations*, *JCAP* **09** (2024) 012, [[arXiv:2404.18475](#)].
- [82] T. Shinohara, T. Suyama, and T. Takahashi, *Angular correlation as a novel probe of supermassive primordial black holes*, *Phys. Rev. D* **104** (2021), no. 2 023526, [[arXiv:2103.13692](#)].
- [83] V. De Luca, G. Franciolini, A. Riotto, and H. Veermäe, *Ruling Out Initially Clustered Primordial Black Holes as Dark Matter*, *Phys. Rev. Lett.* **129** (2022), no. 19 191302, [[arXiv:2208.01683](#)].
- [84] T. Shinohara, W. He, Y. Matsuoka, T. Nagao, T. Suyama, and T. Takahashi, *Supermassive primordial black holes: a view from clustering of quasars at  $z \sim 6$* , [arXiv:2304.08153](#).
- [85] M. Y. Khlopov, S. G. Rubin, and A. S. Sakharov, *Primordial structure of massive black hole clusters*, *Astropart. Phys.* **23** (2005) 265, [[astro-ph/0401532](#)].
- [86] Y. Tada and S. Yokoyama, *Primordial black holes as biased tracers*, *Phys. Rev. D* **91** (2015), no. 12 123534, [[arXiv:1502.01124](#)].
- [87] S. Young and C. T. Byrnes, *Signatures of non-gaussianity in the isocurvature modes of primordial black hole dark matter*, *JCAP* **04** (2015) 034, [[arXiv:1503.01505](#)].
- [88] R. van Laak and S. Young, *Primordial black hole isocurvature modes from non-Gaussianity*, [arXiv:2303.05248](#).
- [89] C. T. Byrnes, K. Koyama, M. Sasaki, and D. Wands, *Diagrammatic approach to non-Gaussianity from inflation*, *JCAP* **11** (2007) 027, [[arXiv:0705.4096](#)].
- [90] G. Franciolini, A. Iovino, Junior., V. Vaskonen, and H. Veermäe, *Recent Gravitational Wave Observation by Pulsar Timing Arrays and Primordial Black Holes: The Importance of Non-Gaussianities*, *Phys. Rev. Lett.* **131** (2023), no. 20 201401, [[arXiv:2306.17149](#)].